


S-allylmercapto-*N*-acetylcysteine protects bone cells from oxidation and improves femur microarchitecture in healthy and diabetic mice

Reem Abu-Kheit¹, Shlomo Kotev-Emeth¹, Sahar Hiram-Bab², Yankel Gabet²  and Naphtali Savion¹ 

¹Department of Human Molecular Genetics and Biochemistry and Goldschleger Eye Research Institute, Sackler Faculty of Medicine, Tel Aviv University, Tel Aviv 6997801, Israel; ²Department of Anatomy and Anthropology, Sackler Faculty of Medicine, Tel Aviv University, Tel Aviv 6997801, Israel

Corresponding author: Naphtali Savion. Email: eyeres@tauex.tau.ac.il

Impact Statement

Oxidative stress is suggested to adversely affect bone quality and mechanical strength. This study demonstrates the antioxidant protective effect of S-allylmercapto-*N*-acetylcysteine (ASSNAC) on bone tissue. ASSNAC protects cultured bone marrow stromal cells (BMSCs) from advanced glycation end-products (AGEs)-induced cytotoxicity by attenuating reactive oxygen species (ROS) production. In healthy mice treated with ASSNAC, an increase in the number and percentage of mesenchymal cells in the BM and in glutathione content was observed. Furthermore, in obese/diabetic (db/db) mice, which demonstrate significant deterioration of bone quality associated with compromised trabecular bone and growth plate microarchitecture, the treatment with ASSNAC improves the microarchitecture of the femur bone. These findings suggest the potential of ASSNAC to attenuate the deterioration of bone tissue microarchitecture of adult healthy and diabetic female mice.

Abstract

Oxidative stress is involved in the deterioration of bone quality and mechanical strength in both diabetic and aging adults. Therefore, we studied the ability of the antioxidant compound, S-allylmercapto-*N*-acetylcysteine (ASSNAC) to protect bone marrow stromal cells (BMSCs) from advanced glycation end-products (AGEs) cytotoxicity and improve bone microarchitecture of adult healthy and obese/diabetic (db/db) female mice. ASSNAC effect on AGEs-treated cultured rat BMSCs was evaluated by Neutral Red and XTT cell survival and reactive oxygen species (ROS) level assays. Its effect on healthy (C57BL/6) and obese/diabetic (C57BLKS/J Lepr^{db+/+}; db/db) female mice femur parameters, such as (1) number of adherent BMSCs, (2) percentage of CD73⁺/CD45⁻ cells in bone marrow (BM), (3) glutathione level in BM cells, and (4) femur microarchitecture parameters by microcomputed tomography, was studied. ASSNAC treatment protected BMSCs by significantly decreasing AGEs-induced ROS production and increasing their cellular resistance to the cytotoxic effect of AGEs. ASSNAC treatment of healthy female mice (50 mg/kg/day; i.p.; age 12–20 weeks) significantly increased the number of BMSCs (+60%), CD73⁺/CD45⁻ cells (+134%), and glutathione level (+110%) in the femur bone marrow. Furthermore, it increased the femur length (+3%), cortical diameter (+3%), and cortical areal moment of inertia (Ct.MOI; +10%) a surrogate for biomechanical strength. In db/db mice that demonstrated a compromised trabecular bone and growth plate microarchitecture, ASSNAC treatment restored the trabecular number (Tb.N, +29%), bone volume fraction

(Tb.BV/TV, +130%), and growth plate primary spongiosa volumetric bone mineral density (PS-vBMD, +7%) and thickness (PS-Th, +18%). In conclusion, this study demonstrates that ASSNAC protects bone marrow cells from oxidative stress and may improve bone microarchitecture in adult healthy and diabetic female mice.

Keywords: Bone marrow stromal cells, microcomputed tomography, osteoporosis, oxidative stress, diabetes type 2

Experimental Biology and Medicine 2022; 247: 1489–1500. DOI: 10.1177/15353702221095047

Introduction

Bone is constantly renewed by a delicate balance between osteoblastic bone formation and osteoclastic bone resorption and this balance is pivotal for the maintenance of integrity and function of the skeletal system. Excessive bone resorption or inadequate bone formation during bone remodeling

may result in osteoporosis associated with skeletal fragility.¹ The bone marrow (BM) compartment is rich in hematopoietic and stromal cells (BMSCs)² that have a self-renewal capacity and the potential to differentiate into osteoblasts, adipocytes, chondrocytes, myocytes, fibroblasts, and endothelial cells.^{3–5} Essential characteristics of BMSCs include plastic adherence when maintained in standard culture conditions, expression

of CD73 by >95% of the cells, and low expression (<2%) of CD45 (pan-leukocyte marker).^{6,7}

Oxidative stress is associated with reduced activity of cellular antioxidant defense mechanisms and/or increase in environmental- or cellular metabolism-derived free radicals, such as reactive oxygen species (ROS). It is implicated in the development and progression of various diseases, including cancer, neurodegenerative diseases, rheumatoid arthritis, chronic inflammation, autoimmune diseases, renal failure, atherosclerosis, ischemia/reperfusion injury, aging, diabetes mellitus,^{8,9} and osteoporosis.^{10,11} Oxidative stress may also play a central role in the pathogenesis of diabetes-associated osteoporosis.^{12,13}

Protection from the deleterious effect of ROS is achieved by antioxidants that are classified according to their mechanism of action, either by direct scavenging of free radicals or by indirect mechanisms increasing the endogenous cellular antioxidant defense by the activation of nuclear factor-erythroid 2-related factor 2 (Nrf2).¹⁴ Under oxidative stress conditions, Nrf2 translocates to the nucleus, where it induces the expression of Phase-II detoxifying and antioxidant enzymes, and the biosynthesis of glutathione, the major intracellular redox buffer, thereby protecting cells from oxidative stress.¹⁵

The established involvement of oxidative stress in the progression of age-related degenerative diseases^{16,17} triggered the search for compounds capable of controlling the oxidant/antioxidant balance that may effectively delay degenerative processes.¹⁸ These compounds include vitamins and polyphenols,¹⁴ *N*-acetyl-*L*-cysteine (NAC), and its derivative *N*-acetylcysteine amide^{19,20} and luteolin,²¹ all of which acting directly or indirectly as ROS scavengers. Furthermore, the natural antioxidants polyphenols and anthocyanins protect cultured bone cells and support their osteogenic differentiation²² and protect against bone loss in osteoporosis mouse model.^{23,24} Nutraceutical antioxidants that may serve as protective agents were recently reviewed by Kelsey *et al.*¹⁴ and divided into molecules that directly scavenge free radicals or augment the endogenous cellular antioxidant defense mechanisms by the activation of Nrf2.²⁵

This study explores the role of our newly developed compound, *S*-allylmercapto-*N*-acetyl-cysteine (ASSNAC) in bone metabolism. ASSNAC is a conjugate of *S*-allylmercaptan, the hydrophobic moiety of allicin, rendering the molecule cell permeability and upregulating glutathione level,²⁶ and NAC, a supplier of cysteine, the limiting precursor in glutathione biosynthesis. Our previous *in vitro* studies have shown that ASSNAC undergoes a thiol exchange reaction with free cysteine residues on the oxidative stress sensor of Keap1, resulting in the release of Nrf2 from its complex with Keap1 and its translocation into the nucleus.²⁷ In parallel, the free NAC released throughout the process is utilized for glutathione biosynthesis. Thus, ASSNAC plays a dual role, activating Nrf2 and supplying cysteine. Nrf2 nuclear translocation activates the expression of Phase-II detoxifying and antioxidant enzymes, including the cysteine transporter (xCT) and glutathione synthesis enzymes, leading to an increase in cellular glutathione, altogether protecting vascular endothelial²⁷ and nerve cells²⁸ from ROS-induced oxidative stress. *In vivo* studies further demonstrated a protective role for ASSNAC against oxidative stress, as it

prevents the death of *Caenorhabditis elegans* exposed to lethal concentrations of H₂O₂,²⁹ attenuates the clinical symptoms of experimental autoimmune encephalomyelitis, serving as a multiple sclerosis mouse model,²⁸ and ameliorates elastase-induced chronic obstructive pulmonary disease in mice.³⁰

Thus, in this study, we explored the ability of ASSNAC to protect BMSCs from the diabetes-associated AGEs-induced cytotoxic effect *in vitro* and improve bone microarchitecture in adult healthy and diabetic mice *in vivo*.

Materials and methods

ASSNAC was synthesized as previously described.²⁷ Briefly, cold sodium thiosulfate and allyl bromide mixed to form allylthiosulfate was further mixed with a cold solution of NAC (at pH 8.0). The resulting ASSNAC extracted at room temperature (at pH 3.0) by *t*-Butyl methyl ether that was evaporated under vacuum conditions, resulting in the formation of ASSNAC in the form of yellowish oil crystals. The purity of the preparation was assessed by high-performance liquid chromatography (HPLC) using a C:18 hydrophobic column and ASSNAC appeared as a major peak representing 96.8% of the loaded material at a retention time of 6.23 min. One contaminating peak of a less hydrophobic material at a retention time of 3.91 min, representing 3.2% of the loaded material, was also detected. To prepare an aqueous stock solution, 100 mg ASSNAC dissolved in 8.48 mL DDW and 2.12 mL Na₃PO₄ (0.2 M). The resulting ASSNAC solution (40 mM) in phosphate buffer (40 mM; pH=7.4) was further diluted in phosphate-buffered saline (PBS) and kept at 4°C.

However, 5-Sulfosalicylic acid, oxidized glutathione (GSSG), D-glycolaldehyde, D-ribose, bovine serum albumin (BSA; endotoxin free), and Neutral Red dye were purchased from Sigma (St. Louis, MO, USA). Alpha-modified Eagle's minimal essential medium (α MEM), antibiotics, glutamine, trypsin (0.25%)/EDTA (0.02%), bovine fibronectin, and fetal calf serum (FCS) were from Biological Industries (Beit Haemek, Israel). Tissue culture dishes were from Nunc (Roskilde, Denmark). PE-conjugated anti-CD73 antibody was from R&D Systems (Minneapolis, MN, USA), and Pacific BLUE-conjugated anti-CD45 antibody was from Biogen (San Diego, CA, USA).

Cell culture

A rat long-term cell line of BMSCs with osteogenic potential prepared in our laboratory³¹ was grown in α MEM supplemented with FCS (15%), glutamine (2 mM), and antibiotics (penicillin [100 U/mL], streptomycin [100 μ g/mL], and nystatin [12.5 U/mL]) (Growth medium).

Preparation of advanced glycation end-products

Advanced glycation end-products (AGEs) were prepared as previously described³² using glycolaldehyde and ribose as reducing reagents, resulting in the formation of Gly-BSA and Rib-BSA, respectively. Briefly, BSA (50 mg/mL) was incubated at 37°C under sterile conditions with D-ribose or D-glycolaldehyde (0.1 M) in a phosphate buffer (0.2 M; pH 7.4) for 7 days followed by dialysis against PBS (pH 7.4) at

4°C and the prepared AGEs, Rib-BSA and Gly-BSA, respectively, were collected and sterilized by filtration. BSA treated similarly but without the reducing agents was used as a control. The reducing level of Rib-BSA and Gly-BSA was visible as a change in the BSA solution color from white to brown-yellow and brown-dark brown, respectively.

Cell survival assay

Rat BMSCs grown in fibronectin-coated (5 µg/mL) 24-well plates up to 70%–80% confluence were washed, exposed to medium containing 0.5% FCS in the presence or absence of ASSNAC (0.2 mM) for 18 h, and further incubated in the presence or absence of Rib-BSA and Gly-BSA for 6 or 24 h. The number of viable cells was determined by the Neutral Red staining method as previously described.³³ Briefly, cultures were washed, incubated in Dulbecco's Modified Eagle Medium (DMEM) containing Neutral Red solution (1%; 2 h; 37°C), and washed, and the Natural Red staining in the cell layer, representing cell survival, was extracted with the Sorenson solution and read on a colorimetric plate reader at a 550 nm wavelength. The number of viable cells was further tested by the XTT kit (Biological Industries Ltd., Beit Haemek, Israel). Briefly, cells were cultured in 100 µL medium/well in a flat 96-well plate and treated as described for 24 h. Cultures were further incubated for 2 h with freshly prepared XTT reagent and activation solution (50 µL per well), and the absorbance was read against a background control (culture medium without cells) with an enzyme-linked immunosorbent assay (ELISA) reader at 490 nm.

ROS measurement

Intracellular ROS levels were examined using the H₂DCF-DA kit (PromoCell, Heidelberg, Germany) according to the manufacturer's instructions. The fluorescence intensity was measured using a fluorescence plate reader (Bio-Tek) at Ex/Em = 495/527 nm.

Animals

Animal source and maintenance

C57BL/6J-Rcc healthy wild-type (WT) female mice (7 weeks old) were purchased from Envigo Ltd. (Rehovot, Israel) and C57BLKS/J Lepr^{db+/−} from the Jackson Laboratory (Bar Harbor, Maine, USA). Homozygote C57BLKS/J Lepr^{db+/+} female mice (db/db; diabetic) were obtained by in-house breeding followed by genotype characterization. Animals were housed at an ambient temperature of 23°C and a 12-h light–dark cycle with water and food ad libitum. Animal experiments were approved by the Tel Aviv University Institutional Animal Care and Use Committee (Approval No. M-14-020) and carried out in accordance with the National Institutes of Health guide for the care and use of Laboratory animals.

Animal treatment

Mice were injected, starting at the age of 12 weeks, with either ASSNAC at a dose used in our previous study²⁸ (i.p.; 50 mg/kg/day dissolved in 0.1 mL PBS) or with PBS

alone (i.p.; 0.1 mL), as control group, five times per week for 8 weeks. Mice health and weight monitored weekly and every 2 weeks, respectively. A 15% weight loss and loss of ability to ambulate (inability to access food or water) were indicators for a deteriorating body condition and the need to immediately kill these mice due to humane reasons. At the end of treatment, mice (20 weeks old) were killed in a CO₂ atmosphere and the femurs were collected.

Animal groups

The original aim of this study was to explore the effect of ASSNAC on BM cells of healthy and diabetic mice. The first feasibility experiment included 10 healthy and 4 db/db female mice that were randomly divided into two treatment groups, treated either with PBS (healthy – 8 and db/db – 2 mice) or with ASSNAC (healthy – 2 and db/db – 2 mice). At the end of the treatment, BM cells were harvested from the femurs of healthy mice; however, our attempts to harvest BM cells from db/db mice femurs failed due to the brittleness of their bones. This unexpected observation limited our study to BM cells of healthy mice. However, the observed brittleness of the diabetic mice femur led us to modify the aim of the study and to explore the effect of ASSNAC on the microarchitecture of the femur bone of both healthy and db/db mice. Consequently, the second experiment, included 16 healthy and 8 db/db female mice that were randomly divided into two treatment groups, treated either with PBS (healthy – 8 and db/db – 4 mice; 1 db/db mouse died, finally *n* = 3) or with ASSNAC (healthy – 8 and db/db – 4 mice).

Femur collection

At the end of the treatment, one femur from each mouse was taken for microcomputed tomography (µCT) analysis and the other femur from each healthy mouse was used for BM cells isolation. The BM-collected cells were counted and subjected to adhesion assay. Aliquots of BM cells were also used for fluorescence-activated cell sorting (FACS) analysis (*n* = 5 and *n* = 6 for control and ASSNAC-treated mice, respectively) and for glutathione determination (*n* = 3).

BM cells collection

Dissected femurs were washed three times (10 min each) in αMEM containing antibiotic (10-fold of growth medium concentration). BM cells were flushed out with growth medium by insertion of a 25G needle into the femur using a 1 mL syringe. Red blood cells in the collected samples were lysed by 10-min incubation in lysis buffer.³⁴ BM cells were collected by centrifugation, re-suspended in 1 mL growth medium and counted using a Bright-Line Hemocytometer. The samples were used for cell adhesion assays (80% of cells in each femur), FACS analysis, and glutathione determination (10% of cells for each assay).

BM cells adhesion assay

Freshly collected BM cells suspended in 10 mL growth medium were incubated in 10-cm tissue culture plates (37°C, 10% CO₂) for 48 h, then washed and attached cells (BMSCs) were collected using a trypsin/EDTA solution and counted.

Glutathione determination

Aliquots of BM cells were centrifuged and pellets were lysed in HCl (10 mM), followed by three cycles of freezing and thawing, and proteins were precipitated by the addition of 5-Sulfosalicylic acid (10%) followed by centrifugation (10,000g). Supernatants were used for glutathione determination by the Anderson recycling method³⁵ using 96-well plates. Results were determined at 412 nm in an Elisa Reader (ELx808; Bio-Tek Instruments Inc., Winooski, VT, USA) and presented as nmole GSH per 10⁶ cells.

Expression of CD45 and CD73 cell surface markers

Expression of hematopoietic cells marker (CD45) and BMSCs marker (CD73)³⁶ was studied using fluorescence-labeled antibodies. Aliquots of freshly collected BM cells were centrifuged, re-suspended in FACS buffer (PBS without calcium and magnesium containing 1% FCS, 0.5 mM EDTA, and 0.1% sodium azide) and aliquots of 0.5 × 10⁶ cells were incubated with the antibodies in the dark (30 min; 4°C), washed with FACS buffer by centrifugation, fixed in 2% paraformaldehyde (overnight), and analyzed by FACS Calibur (Becton Dickinson, Franklin Lakes, NJ, USA). Fluorescence-labeled rat IgGs isotype controls were used to determine background fluorescence (cut-off of less than 0.5% false positive). Collected events (10⁴/sample) were analyzed by the Flowing Software (version 2.5.1, University of Turku, Finland).

Femur μ CT analysis

Dissected femurs were fixed in paraformaldehyde solution (4%) for 48 h, washed, transferred to 70% ethanol, and analyzed on a μ CT50 system (Scanco Medical AG, Switzerland) as previously reported.³⁷ Briefly, whole femurs were scanned at a 10 μ m nominal isotropic resolution, with 90 kV energy, 88 μ A intensity, and 1000 projections with a 1000 ms integration time. A gaussian filtration (sigma = 0.8, support = 1) and threshold (160 permil for trabecular bone and 224 permil for cortical bone) were applied to the tomographic volumes. The femur trabecular bone parameters were measured in the secondary spongiosa of the distal femoral metaphysis defined as a 3 mm height volume ending distally at the proximal-most border of the primary spongiosa (PS) (calcified part of the growth plate). The following parameters were analyzed: femur length, trabecular bone volume fraction (Tb.BV/TV), trabecular number (Tb.N), spacing (Tb.Sp), and thickness (Tb.Th). The cortical bone parameters were determined in a 1 mm height ring located at the mid-diaphysis and consisted of cortical thickness (Ct.Th; direct measure), moment of inertia (Ct.MOI; areal), cortical bone area fraction (Ct.BA/TA), and mid-diaphyseal diameter (Ct.Dia.Dia; based on the cross-sectional area). In addition, to determine the effect of diabetes and ASSNAC treatment on the epiphyseal growth plate, we delineated the unmineralized and mineralized parts of the growth plate. The former will be referred as "cartilage" (Cart) and the latter, which comprises both the mineralizing cartilage and the PS, will be herein referred to as the PS. After manual delineation, we refined the borders of each part using segmentation (below and above 100 permil of

maximal gray values for the cartilage and PS, respectively). In each compartment, we measured the mean thickness of the PS and Cart (PS-Th; Cart-Th) layers and the volumetric bone mineral density (PS-vBMD). In the PS, we also measured the bone volume fraction (PS-BV/TV, which is also the inversed ratio of the porosity).

Statistical analysis

Results are presented as mean \pm SD. Statistical analysis was tested by two-way ANOVA with Bonferroni *post hoc* test (multiple groups), two-tailed Mann-Whitney test or Student's *t*-test (for paired comparisons). Differences at $p \leq 0.05$ were considered statistically significant and differences at the range of $0.10 \geq p \geq 0.05$ were considered close to significant.

Results

ASSNAC attenuates AGEs-induced cytotoxicity in cultured rat BMSCs

The previously observed lack of ASSNAC cytotoxicity (up to 2.0 mM and optimal activity at 0.2 mM) in vascular endothelial cells²⁷ was confirmed in a preliminary experiment with rat BMSCs cultures. Consequently, to test the protective effect of ASSNAC against AGEs-induced cytotoxicity, rat BMSCs cultures were either not pretreated or pretreated with ASSNAC (0.2 mM; 18 h), exposed to Rib-BSA or Gly-BSA for 6 h (Figure 1(A)) or 24 h (Figure 1(B), (D), and (E)) and analyzed for cell survival. Exposure to Rib-BSA or Gly-BSA at concentrations of 2 mg/mL for 6 h or 0.5 and 1.0 mg/mL for 24 h, resulted in significant cytotoxicity of up to 80–90% (Figure 1(A)) or 90–100% (Figure 1(B)), respectively. Cells treated with un-glycated albumin (BSA) or H₂O₂ were used as negative and positive controls and demonstrated no cytotoxicity (96% cell survival) or significant cytotoxicity (42% cell survival), respectively; ASSNAC pretreatment significantly protected the H₂O₂-treated cells (76% cell survival) (Figure 1(E)). The cytotoxic effect of Rib-BSA and H₂O₂ and the protective effect of ASSNAC were also confirmed using the XTT cell survival assay (Figure 1(D)). In summary, ASSNAC significantly protected BMSCs as reflected by an almost complete prevention of the cytotoxic effect of Rib-BSA, Gly-BSA, and H₂O₂.

ASSNAC attenuates Rib-BSA-induced ROS production

Rib-BSA-treated rat BMSCs demonstrated a significant increase in ROS production, which was significantly attenuated by ASSNAC pretreatment (45% reduction) (Figure 1(C)).

The weight and blood glucose level of healthy and diabetic mice

The weight and blood glucose level of 12- and 20-week-old mice from the second experiment is presented in Table 1. Blood glucose levels were significantly higher (about threefold) in db/db compared to healthy mice and were not affected by ASSNAC treatment in either group. The weight of db/db mice was significantly higher (about twofold)

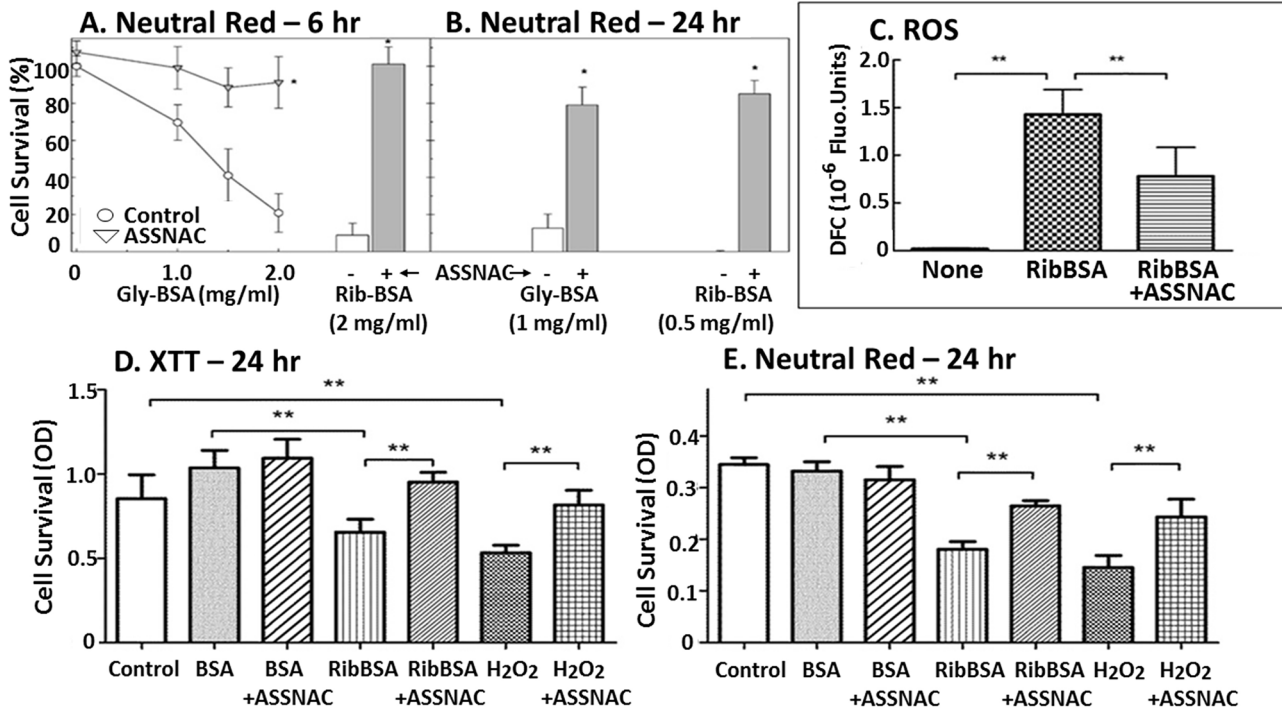


Figure 1. Effect of ASSNAC on the survival and ROS level of AGEs-treated BMSCs. Rat BMSCs treated with or without ASSNAC (0.2 mM) for 18 h were further exposed to Rib-BSA and Gly-BSA at the indicated concentrations for (A) 6 h or (B) 24 h. Control and ASSNAC-treated cultures were further exposed to untreated BSA, Rib-BSA (2 mg/mL), or H₂O₂ (50 μM) for 24 h (D and E). At the end of the treatment, cultures were washed and cell survival determined by the Neutral Red assay (A, B, and E) and by XTT kit (D). Cultures treated without or with ASSNAC (0.2 mM) for 18 h were further exposed to Rib-BSA (2 mg/mL) for 24 h, while control cultures were not treated (None) followed by ROS determination (C). The results are presented as mean ± SD (a. n=2; b. n=2; c. n=8; d. n=6; e. n=4). Significance of difference was tested in (A) and (B) by the two-way ANOVA with Bonferroni *post hoc* test; (*)p ≤ 0.01; and in (C), (D), and (E) by two-tailed Mann-Whitney test; (**)p ≤ 0.001.

Table 1. Blood glucose and weight.

Treatment	A. Glucose		B. Weight	
	Mean ± SD; mg/dL		Mean ± SD; grams	
	12 weeks	20 weeks	12 weeks	20 weeks
WT	138 ± 33	133 ± 14	18.5 ± 2.3	18.3 ± 1.0
WT + ASSNAC	139 ± 26	144 ± 15	18.2 ± 1.8	19.8 ± 1.2**#
Db/db	393 ± 155*	459 ± 105*	41.3 ± 1.5*	43.3 ± 4.0*
Db/db + ASSNAC	449 ± 154*	495 ± 167*	41.5 ± 12.4*	43.5 ± 11.1*

Number of mice per group: WT – 8; WT + ASSNAC – 8; Db/Db – 3; Db/Db + ASSNAC – 4.

*Significant difference – db/db versus WT mice.

**Significant difference – WT + ASSNAC versus WT mice.

#Significant difference – 20 versus 12 weeks.

compared to healthy mice, while ASSNAC treatment significantly increased the weight of healthy mice (+8.8%) but not that of db/db mice.

ASSNAC increases BMSCs number and the glutathione level in mouse femur BM cells

A 20-week old healthy female mouse femur contains about 17 × 10⁶ BM cells, 2.4% of which are adherent BMSCs (Figure 2(A) and (B)). ASSNAC treatment of healthy female mice had no effect on the femur BM cell number (Figure 2(A)); however, it significantly increased (+60%) the femur adherent BMSCs number (Figure 2(B)). In addition, femur BM cells collected from ASSNAC-treated mice demonstrated a

significant increase in glutathione level (+110%) compared to that of cells collected from control mice (Figure 2(C)).

ASSNAC affects BM cell population phenotype

BM cells harvested from femurs of control (Figure 3(A)) or ASSNAC-treated (Figure 3(B)) healthy mice were stained, or not stained, with a PE-conjugated anti-CD73 or an isotype control antibody and analyzed by FACS. The scatter histograms of cells stained or not stained with the isotype control antibody overlapped, indicating lack of non-specific staining.

Analysis of histograms presented in Figure 3(A) and (B) revealed an ASSNAC-induced significant increase (+134%)

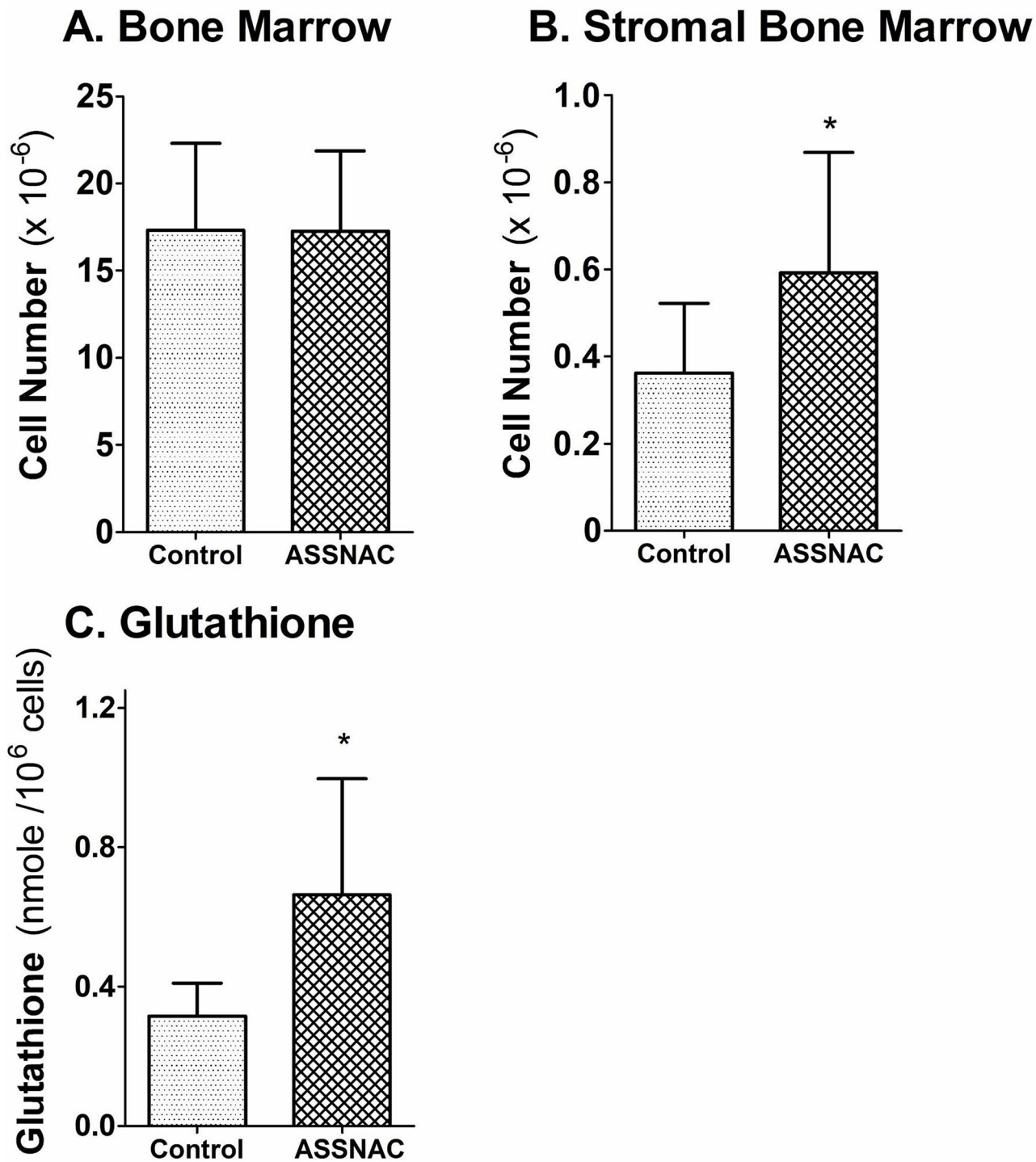


Figure 2. Effect of ASSNAC on cell number and glutathione level in femur BM cells. BM cells collected from femurs of healthy female mice either untreated (control; $n = 16$) or ASSNAC-treated ($n = 10$) were counted (A) and plated in tissue culture plates for 48 h and then the adherent BMSCs counted (B). BM cells collected from femurs of healthy female mice either untreated (control; $n = 3$) or ASSNAC-treated ($n = 3$) were subjected to glutathione determination (C). Data are presented as mean \pm SD and significance of difference was tested by two-tailed Student's *t*-test; (*) $p \leq 0.05$.

in the population of CD73-positive cells as compared to that of control cells ($16.2 \pm 4.2\%$ versus $6.9 \pm 4.5\%$, respectively) (Figure 3(C)).

Anti-CD73 and anti-CD45 double staining of BM cells from control and ASSNAC-treated healthy mice revealed a low percentage of double stained cells ($0.98 \pm 0.80\%$ and $0.48 \pm 0.43\%$, respectively), suggesting that the majority of

the CD73-positive cells are CD45-negative, indicating their stromal nature.

ASSNAC improves femur bone microarchitecture in healthy and db/db mice

Femurs of WT healthy female mice treated with ASSNAC or PBS (control) for 8 weeks were analyzed by μ CT. ASSNAC

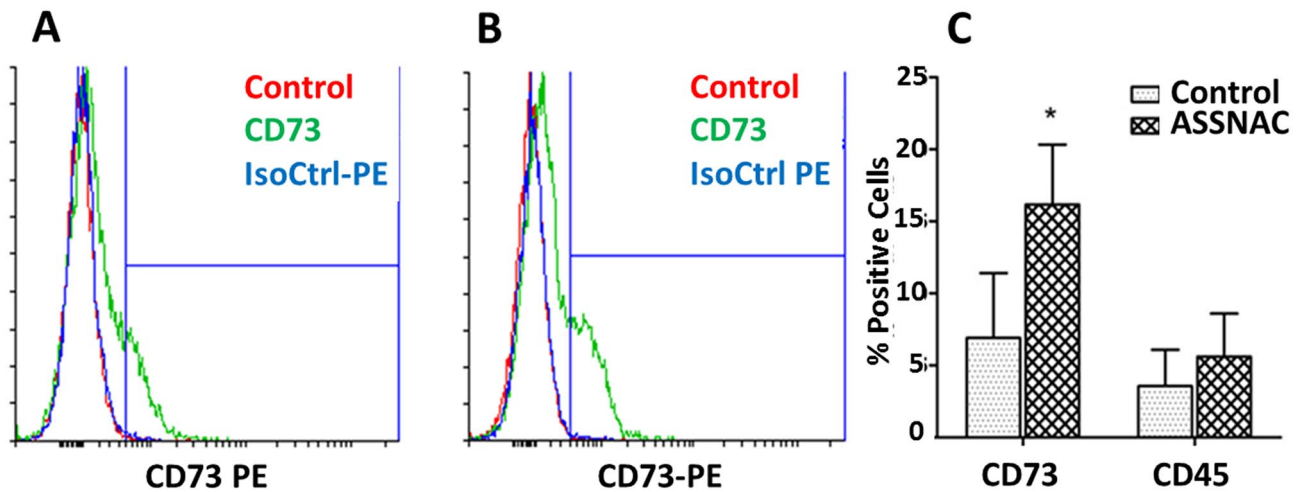


Figure 3. Effect of ASSNAC on the percent of BM cells expressing CD73 and CD45. Flow cytometry fluorescence scatter histogram of BM cells of non-treated (A) and ASSNAC-treated (B) mice are presented (representative experiment). The cells were either not stained (red line) or stained with anti-CD73-PE (green histogram) or an isotype control antibody (blue histogram). BM cells of both animal treatments were stained with anti CD73-PE and CD45-PB antibodies and the percentage of positive cells \pm SD in each treatment is presented (C). To calculate the percentage of positive cells, a gate of up to 0.5% false positive was set. Significance of difference was tested by two-tailed Student's *t*-test; (*) $p \leq 0.05$ (control $n=5$; ASSNAC $n=6$).

significantly increased femur bone length (+3%) and diameter (+3%), improved the estimated cortical bone mechanical strength based on the improved Ct.MOI (+10% [areal]) and close to significant increase in cortical thickness (+9%; $p=0.098$), while trabecular parameters were not affected (Figure 4(A)). db/db mice demonstrated a significant deterioration of the bone microarchitecture compared to healthy mice (Figure 4(A) and (B) and Figure 5), including decreased Tb.BV/TV (-61%), Tb.Th (-29%), Ct.MOI (-18%), and close to significant decrease in Ct.Th (-23%; $p=0.056$) and Ct.BA/TA (-20%; $p=0.080$). Diabetic mice exhibited also a close to significant decrease in femur length (-8%; $p=0.070$ versus WT). ASSNAC treatment of db/db female mice (Figures 4(B) and 5) significantly increased Tb.N (+29%) and Tb.BV/TV (+130%), the latter to a level similar to healthy mice, demonstrating a significant restoration of the deleterious skeletal effect of diabetes. Other bone parameters impaired in db/db mice were partially improved by ASSNAC treatment (close to significant effect) including decreased Tb.Sp (-29%; $p=0.086$) and increased Tb.Th (+26%; $p=0.065$), Ct.MOI (+10%; $p=0.100$) and bone length (+5%; $p=0.110$). Cortical and trabecular images of control, db/db, and ASSNAC-treated db/db mice presented in Figure 5 demonstrate the compromised bone structure of db/db mice and the ASSNAC-induced partial improvement. Notably, ASSNAC partially restored the trabecular bone volume fraction that was severely reduced in the db/db mice and restored the Ct.Th to values similar to the WT mice.

As ASSNAC treatment significantly increased femur length in healthy mice and a similar trend was demonstrated in db/db mice, we analyzed its effect on the femur epiphyseal growth plate (Figure 6). db/db mice demonstrated significant changes, compared to healthy mice, in PS-BV/TV (+10%) and PS-vBMD (-30%) and PS-Th (-19%). ASSNAC treatment of db/db mice resulted in increased PS-vBMD (+7%; close to significant, $p=0.08$) and PS-Th (+18%; close to significant, $p=0.09$). The thickness of the Cart layer was not

affected by the diabetic phenotype nor by the ASSNAC treatment. The microtomographs of representative images show the thinning of the PS in db/db mice with partial recovery following ASSNAC treatment (Figure 6).

Discussion

Our previous studies in cultured vascular endothelial, nerve cells, and retinal pigment epithelial cells demonstrated the protective effect of ASSNAC against oxidative stress through a unique dual mechanism, including Nrf2 nuclear translocation and cysteine supplementation, which supports glutathione biosynthesis.^{27,28,38} Furthermore, ASSNAC was found to attenuate the clinical symptoms of experimental autoimmune encephalomyelitis in a mouse model.²⁸

In this study, we hypothesized that diabetic-associated oxidative stress may have a deleterious effect on bone metabolism and microarchitecture. Therefore, we tested the ability of ASSNAC to protect cultured BMSCs from the cytotoxicity of the hyperglycemia products, Gly-BSA and Rib-BSA, which were shown to significantly induce ROS production followed by cell death. Indeed, ASSNAC significantly attenuated Gly-BSA- and Rib-BSA-induced ROS production and cell death. This observed protective effect of ASSNAC is similar to the previously described protective effect of NAC against AGEs-induced cell death.³⁹ Although it is not clear whether this protective effect of ASSNAC on BMSCs *in vitro* may suggest a similar protective effect on bone cells *in vivo*, we decided to explore ASSNAC effect in healthy and db/db mice. The animal studies further supported the potential antioxidant effect of ASSNAC on BM cells. BM derived from ASSNAC-treated mice demonstrated an increased number of adherent cells and an increased fraction of CD73⁺/CD45⁺ cells, considered as mesenchymal cells.^{6,36} Furthermore, the observed increase in glutathione level in femur BM cells of ASSNAC-treated healthy mice may augment/improve the antioxidant cellular resistance, resulting in increased BMSCs

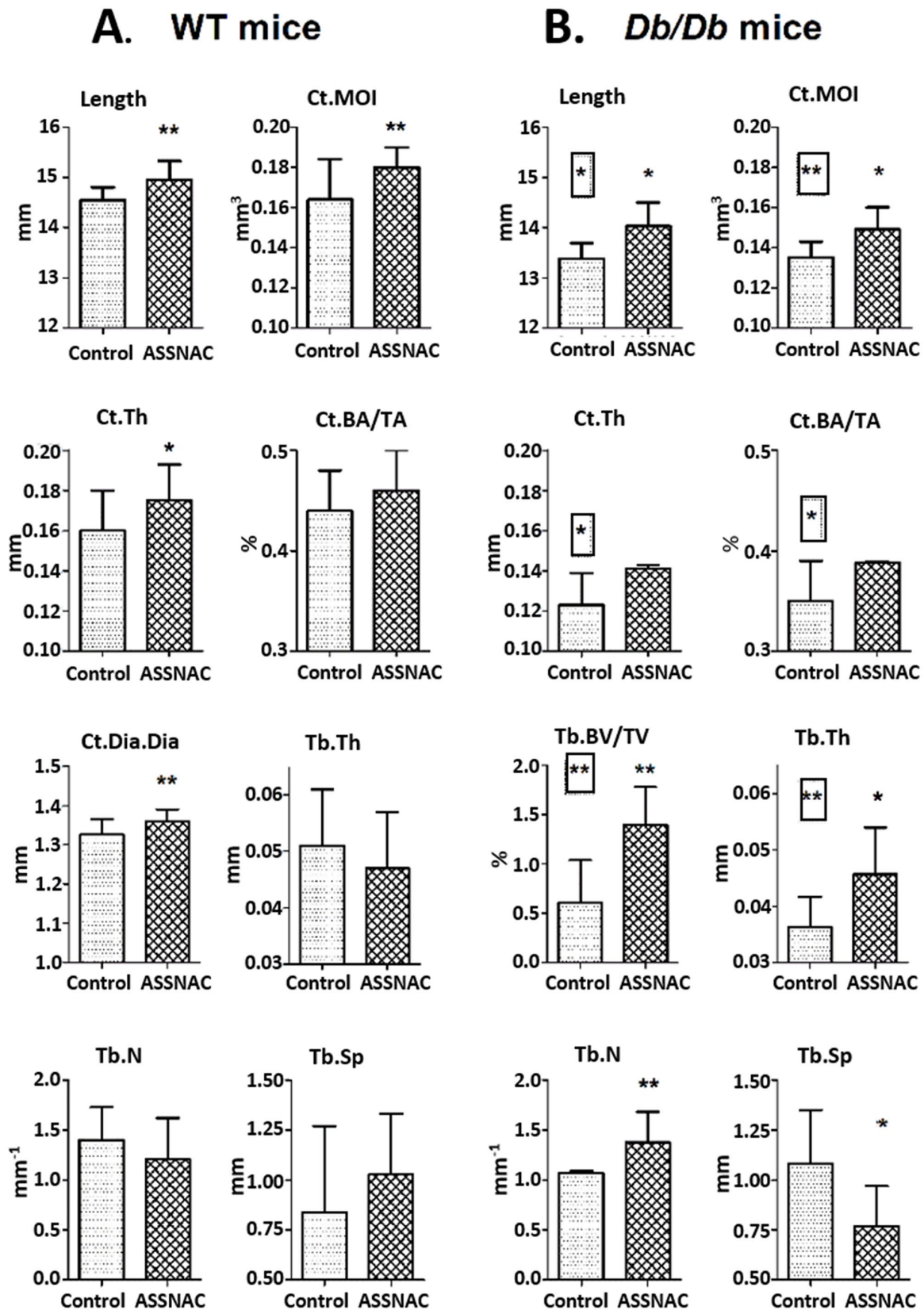


Figure 4. Effect of ASSNAC on μ CT femur trabecular and cortical bone parameters: (A) healthy female mice (WT) treated with PBS (control; $n=8$) or ASSNAC ($n=8$). (B) db/db female mice treated with PBS (control; $n=3$) or ASSNAC ($n=4$). μ CT analysis of the femur included bone length, cortical diameter (Ct.Dia.Dia), thickness (Ct.Th), bone area fraction (Ct.BA/TA), and moment of inertia (Ct.MOI; areal) in the mid-diaphysis and the trabecular bone volume fraction (Tb.BV/TV), number (Tb.N), thickness (Tb.Th), and separation (Tb.Sp) in the distal metaphysis. Data are presented as mean \pm SD. Significant differences were determined by Student's t -test between ASSNAC and control groups (marked by asterisks) and between db/db and healthy mice (marked by asterisks in squares); (***) $p \leq 0.05$, (*) $0.10 \geq p \geq 0.05$.

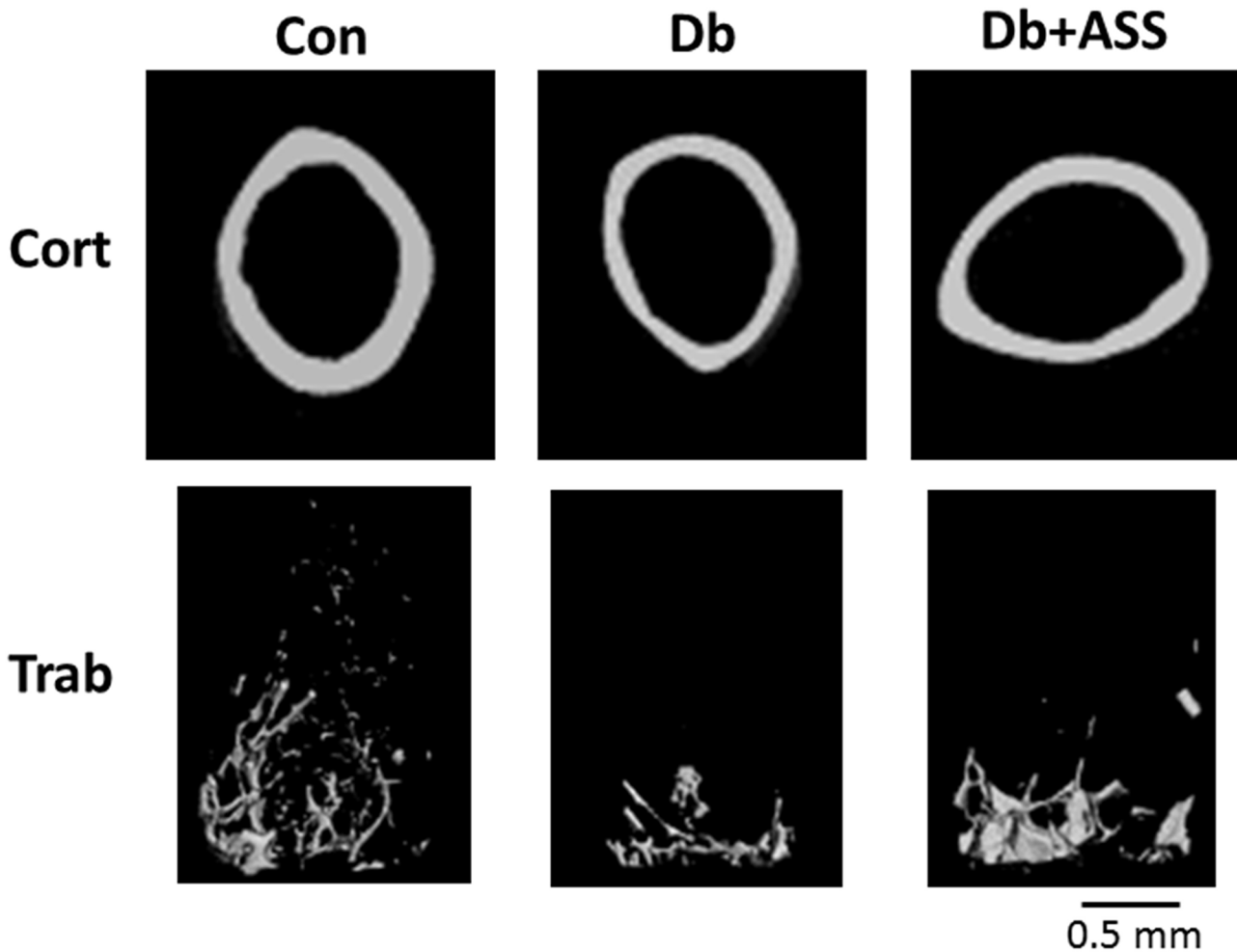


Figure 5. Effect of ASSNAC on femur cortical and trabecular bone architecture of db/db mice. The cortical (Cort) and trabecular (Trab) images of healthy control (Con) and db/db mice without (Db) and with ASSNAC treatment (Db + ASS) are presented. Note that the reduced cortical thickness and trabecular density in the db/db mice were partially rescued in the Db + ASS mice.

number, similarly to the previously reported antioxidant protective effect of curcumin on BM cells in mice.⁴⁰ Thus, we suggest that ASSNAC treatment of healthy female mice may have significantly increased BM antioxidant capacity associated with an increase in the mesenchymal adherent cell population.

Oxidative stress is suggested to play a major role in the progression of diabetes; therefore, we tested the effect ASSNAC on db/db mice and found that it did not affect the elevated blood glucose level. However, we observed an increase in femur length in ASSNAC-treated db/db and healthy mice. This observation may be explained by the fact that unlike in humans, in whom the growth plate closes on maturity, in adult rodents it persists in mature animals.⁴¹ Our results demonstrated an ASSNAC-positive effect on BM cells and an increase in bone femur length of healthy mice. These changes were not accompanied by an increase in relevant growth plate parameters that may explain the increased femur length suggesting that it is probably associated with the increase in body weight in healthy mice. However, the effect of ASSNAC on the growth plate was likely to be transient as the increased PS-vBMD was only close to significance in the μ CT analysis carried out at the

end of the 8-week treatment period. As recently reported for leptin-deficient mice,⁴² our db/db mice demonstrated significant changes in the growth plate μ CT parameters, including deterioration of the PS-vBMD and PS-Th while PS-BV/TV was increased.

Previous studies have reported a compromised trabecular bone microarchitecture with a significantly lower femur Tb.BV/TV and Tb.Th in mice with impaired leptin activity, such as db/db^{43,44} and ob/ob.^{43,45} Our study confirms the significantly lower femur Tb.BV/TV and Tb.Th and further suggests significant deterioration of the Ct.MOI and some close to significant decrease in Ct.Th and Ct.BA/TA in db/db mice.

The effect of ASSNAC treatment differed between healthy and db/db mice. In healthy mice, ASSNAC significantly increased Ct.Dia.Dia and Ct.MOI with a close to significant increase in Ct.Th but it did not affect the trabecular bone compartment. In db/db mice, ASSNAC significantly improved Tb.BV/TV and Tb.N with only close to significant effect on Ct.MOI and Tb.Th. This may suggest a different mechanism of action for ASSNAC in healthy versus diabetic mice. Based on those results, one can speculate that in healthy mice, ASSNAC primarily targets the cortical bone

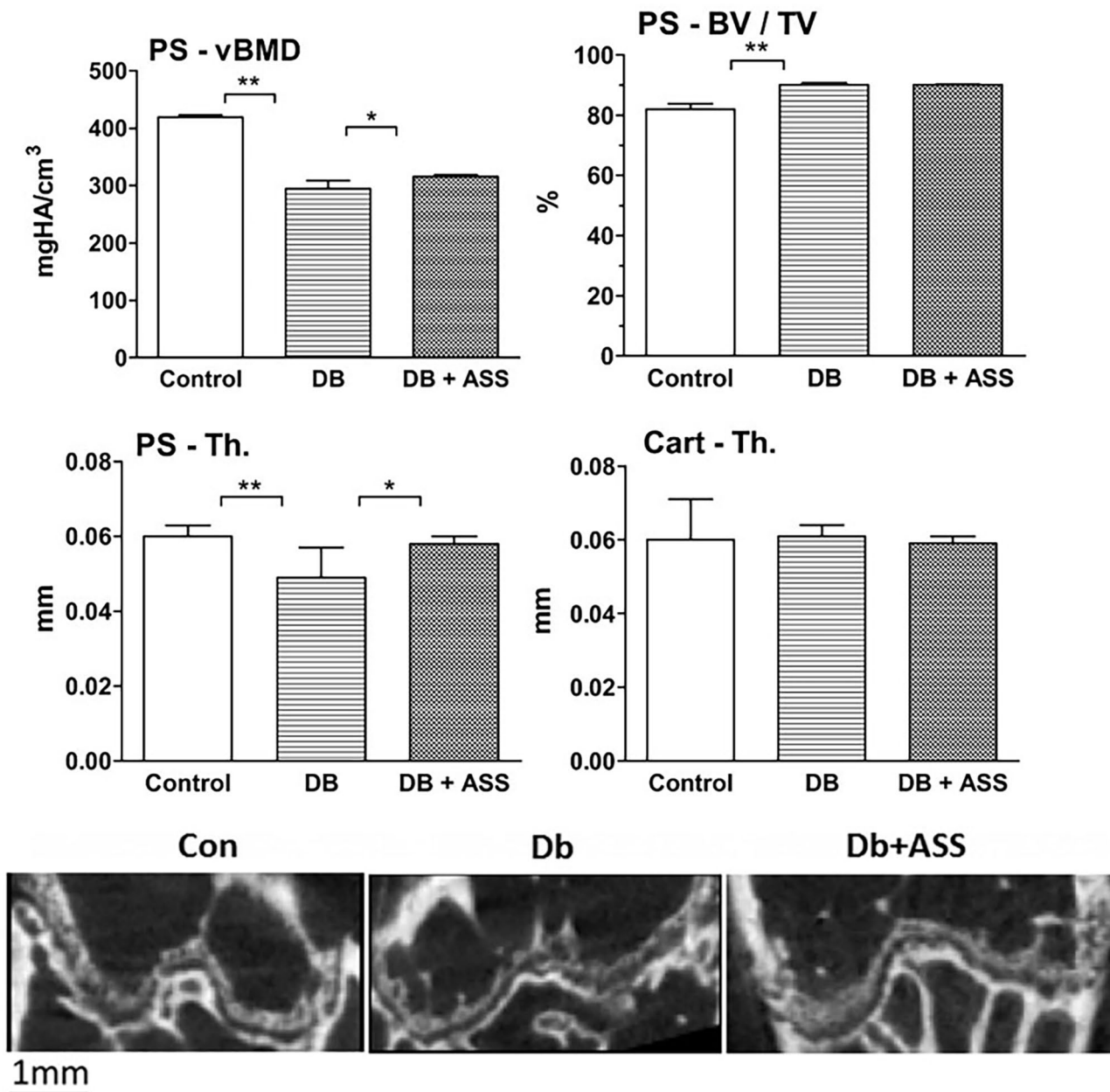


Figure 6. Effect of ASSNAC on the femur growth plate. Femurs of healthy female mice treated with PBS (control; $n=8$) or db/db female mice treated with PBS (DB; $n=3$) or ASSNAC (DB + ASS; $n=4$) were collected. μ CT analysis of the femur growth plate included bone volume fraction (PS-BV/TV), volumetric bone mineral density (PS-vBMD), and thickness (PS-Th) of the PS and cartilage thickness (Cart-Th). Data are presented as mean \pm SD. Significant differences were determined by Student's *t*-test; (**) $p \leq 0.05$, (*) $0.10 \geq p \geq 0.05$. Axial tomographs of growth plate of control (Con) and db/db mice without (Db) or with ASSNAC treatment (Db + ASS) are presented in the lower part of the figure. The cartilage and PS are the lowly (dark) and highly mineralized (light gray) parts of the femoral distal growth plate, respectively.

through an increase in the number of stromal cells, while, in db/db mice, ASSNAC primarily targets the trabecular bone through the neutralization of the diabetes-induced oxidative stress in the BM.

It is suggested that oxidative stress plays a role in altered characteristics of diabetic bone.⁴⁶ The oxidative stress-induced compromised bone structure observed in db/db mice is probably the result of the elevated level of AGEs. Consequently, the observed anti-osteoporotic effect of ASSNAC in the db/db mice might be related to attenuating the AGEs-associated oxidative stress, as observed in our *in vitro* studies. Furthermore, in a previous study in type-1

diabetic rats, a decrease in BM osteoprogenitor cell number, probably due to oxidative stress-induced apoptosis, was observed.⁴⁷ This previous observation in type-1 diabetes may suggest a similar decrease in the BM population in db/db mice that may be attenuated by ASSNAC treatment. Altogether, the protective effect of ASSNAC in diabetic mice described in our study is possibly an anti-oxidative effect and it is in agreement with previous reports demonstrating the attenuation of osteoporosis in a mouse model of Alzheimer by NAC,⁴⁸ the attenuation of type-1 diabetes-induced osteopenia by thioredoxin-1⁴⁹ and the attenuation of sex steroid deficiency-related osteoporosis by flavonoids.⁵⁰

In conclusion, ASSNAC protected cultured BMSCs from AGEs-induced cytotoxicity by attenuating ROS production and increasing the glutathione level in BM cells of healthy mice, suggesting its anti-oxidative protective effect, both *in vitro* and *in vivo*. An increased number and percentage of mesenchymal cells in the BM and an increase in femur length, Ct.Dia.Dia, and Ct.MOI accompanied this effect of ASSNAC in healthy mice. Furthermore, the antioxidative protective effect of ASSNAC in healthy mice may explain its protective effect on the deterioration of bone microarchitecture in db/db mice, demonstrated by the improved femur Tb.N, Tb.BV/TV, and growth plate PS-vBMD and PS-Th. These findings demonstrate the potential of ASSNAC to preserve and prevent deterioration of bone tissue of adult healthy and diabetic female mice.

AUTHORS' CONTRIBUTIONS

All authors participated in the interpretation of the studies and review of the article; N.S. contributed to the study conception and design; R.A.-K., S.K.-E., and S.H.-B. conducted the experiments, data collections, and analysis; N.S. and Y.G. wrote and edited the article.

ACKNOWLEDGEMENTS

This work was conducted in partial fulfillment of the requirements for the MSc degree of Reem Abu-Kheit, Sackler Faculty of Medicine, Tel Aviv University. The authors thank Dr Dov Diller (Casali Institute of Applied Chemistry, the Hebrew University of Jerusalem, Israel) for the ASSNAC synthesis and Prof. Sandu Pitaru (Dental School, Sackler Faculty of Medicine, Tel Aviv University, Tel Aviv, Israel) for the generous donation of db/db mice.

DECLARATION OF CONFLICTING INTERESTS


The author(s) declared the following potential conflicts of interest with respect to the research, authorship, and/or publication of this article: N.S. is one of the inventors of the Patent: compositions comprising S-allylmercapto-N-acetylcysteine (ASSNAC) for upregulation of cellular glutathione level.

FUNDING

The author(s) disclosed receipt of the following financial support for the research, authorship, and/or publication of this article: The μ CT system used in this study has been partly funded by the Israel Science Foundation (Grant no. 1822/12 to Y.G.).

ORCID IDS

Yankel Gabet  <https://orcid.org/0000-0002-7494-0631>

Naphtali Savion  <https://orcid.org/0000-0001-8899-0624>

REFERENCES

- Raisz LG. Pathogenesis of osteoporosis: concepts, conflicts, and prospects. *J Clin Invest* 2005;**115**:3318–25
- Krebsbach PH, Kuznetsov SA, Bianco P, Robey PG. Bone marrow stromal cells: characterization and clinical application. *Crit Rev Oral Biol Med* 1999;**10**:165–81
- Izadpanah R, Trygg C, Patel B, Kriedt C, Dufour J, Gimble JM, Bunnell BA. Biologic properties of mesenchymal stem cells derived from bone marrow and adipose tissue. *J Cell Biochem* 2006;**99**:1285–97
- Bianco P, Robey PG. Marrow stromal stem cells. *J Clin Invest* 2000;**105**:1663–8
- Tuli R, Tuli S, Nandi S, Wang ML, Alexander PG, Haleem-Smith H, Hozack WJ, Manner PA, Danielson KG, Tuan RS. Characterization of multipotential mesenchymal progenitor cells derived from human trabecular bone. *Stem Cells* 2003;**21**:681–93
- Dominici M, Le Blanc K, Mueller I, Slaper-Cortenbach I, Marini F, Krause D, Deans R, Keating A, Prockop Dj, Horwitz E. Minimal criteria for defining multipotent mesenchymal stromal cells. The International Society for Cellular Therapy position statement. *Cytotherapy* 2006;**8**:315–7
- Mohammadzadeh M, Halabian R, Gharehbaghian A, Amirzadeh N, Jahanian-Najafabadi A, Roushander AM, Roudkenar MH. Nrf-2 over-expression in mesenchymal stem cells reduces oxidative stress-induced apoptosis and cytotoxicity. *Cell Stress Chaperones* 2012;**17**:553–65
- West IC. Radicals and oxidative stress in diabetes. *Diab Med* 2000;**17**:171–80
- Schulz JB, Lindenau J, Seyfried J, Dichgans J. Glutathione, oxidative stress and neurodegeneration. *Eur J Biochem* 2000;**267**:4904–11
- Ibáñez L, Ferrándiz ML, Brines R, Guede D, Cuadrado A, Alcaraz MJ. Effects of Nrf2 deficiency on bone microarchitecture in an experimental model of osteoporosis. *Oxid Med Cell Longev* 2014;**2014**:726590
- Basu S, Michaelsson K, Olofsson H, Johansson S, Melhus H. Association between oxidative stress and bone mineral density. *Biochem Biophys Res Commun* 2001;**288**:275–9
- Shanbhogue VV, Mitchell DM, Rosen CJ, Bouxsein ML. Type 2 diabetes and the skeleton: new insights into sweet bones. *Lancet Diab Endocr* 2016;**4**:159–73
- Levin ME, Boisseau VC, Avioli LV. Effects of diabetes-mellitus on bone mass in juvenile and adult-onset diabetes. *New Engl J Med* 1976;**294**:241–5
- Kelsey NA, Wilkins HM, Linseman DA. Nutraceutical antioxidants as novel neuroprotective agents. *Molecules* 2010;**15**:7792–814
- Kensler TW, Wakabayashi N, Biswal S. Cell survival responses to environmental stresses via the Keap1-Nrf2-ARE pathway. *Annu Rev Pharmacol Toxicol* 2007;**47**:89–116
- Casetta I, Govoni V, Granieri E. Oxidative stress, antioxidants and neurodegenerative diseases. *Current Pharmaceutical Design* 2005;**11**:2033–52
- Loenn ME, Dennis JM, Stocker R. Actions of “antioxidants” in the protection against atherosclerosis. *Free Rad Biol Med* 2012;**53**:863–84
- Zhang HY, Yang DP, Tang GY. Multipotent antioxidants: from screening to design. *Drug Discov Today* 2006;**11**:749–54
- Radomska-Lesniewska DM, Skopinski P. N-acetylcysteine as an antioxidant and anti-inflammatory drug and its some clinical applications. *Cent Eur J Immunol* 2012;**37**:57–66
- Offen D, Gilgun-Sherki Y, Barhum Y, Benhar M, Grinberg L, Reich R, Melamed E, Atlas D. A low molecular weight copper chelator crosses the blood-brain barrier and attenuates experimental autoimmune encephalomyelitis. *J Neurochem* 2004;**89**:1241–51
- Zhao G, Yao-Yue C, Qin GW, Guo LH. Luteolin from Purple Perilla mitigates ROS insult particularly in primary neurons. *Neurobiol Aging* 2012;**33**:176–86
- Domazetovic V, Marcucci G, Falsetti I, Bilia AR, Vincenzini MT, Brandi ML, Iantomasi T. Blueberry juice antioxidants protect osteogenic activity against oxidative stress and improve long-term activation of the mineralization process in human osteoblast-like SaOS-2 cells: involvement of SIRT1. *Antioxidants* 2020;**9**:125
- Kim B, Lee S-H, Song S-J, Kim WH, Song E-S, Lee J-C, Lee S-J, Han D-W, Lee J-H. Protective effects of melon extracts on bone strength, mineralization, and metabolism in rats with ovariectomy-induced osteoporosis. *Antioxidants* 2019;**8**:306
- Nagaoka M, Maeda T, Chatani M, Handa K, Yamakawa T, Kiyohara S, Negishi-Koga T, Kato Y, Takami M, Niida S, Lang SC, Kruger MC, Suzuki K. A delphinidin-enriched maqui berry extract improves bone metabolism and protects against bone loss in osteopenic mouse models. *Antioxidants* 2019;**8**:386
- Zhang M, An C, Gao Y, Leak RK, Chen J, Zhang F. Emerging roles of Nrf2 and phase II antioxidant enzymes in neuroprotection. *Prog Neurobiol* 2013;**100**:30–47

26. Horev-Azaria L, Eliav S, Izigov N, Pri-Chen S, Mirelman D, Miron T, Rabinkov A, Wilchek M, Jacob-Hirsch J, Amariglio N, Savion N. Allicin up-regulates cellular glutathione level in vascular endothelial cells. *Eur J Nutr* 2009;**48**:67–74
27. Izigov N, Farzam N, Savion N. S-allylmercapto-N-acetylcysteine up-regulates cellular glutathione and protects vascular endothelial cells from oxidative stress. *Free Rad Biol Med* 2011;**50**:1131–9
28. Savion N, Izigov N, Morein M, Pri-Chen S, Kotev-Emeth S. S-allylmercapto-N-acetylcysteine (ASSNAC) protects cultured nerve cells from oxidative stress and attenuates experimental autoimmune encephalomyelitis. *Neurosci Lett* 2014;**583**:108–13
29. Savion N, Levine A, Kotev-Emeth S, Bening Abu-Shach U, Broday L. S-allylmercapto-N-acetylcysteine protects against oxidative stress and extends lifespan in *Caenorhabditis elegans*. *PLoS ONE* 2018;**13**: e0194780
30. Zheng D, Wang J, Li G, An L, Qu Y, Zhang Q, Ye W, Zhao X, Zhao Z. S-allylmercapto-N-acetylcysteine ameliorates elastase-induced chronic obstructive pulmonary disease in mice via regulating autophagy. *Biochem Biophys Res Commun* 2021;**562**:83–8
31. Kotev-Emeth S, Pitaru S, Pri-Chen S, Savion N. Establishment of a rat long-term culture expressing the osteogenic phenotype: dependence on dexamethasone and FGF-2. *Connect Tissue Res* 2002;**43**:606–12
32. Kume S, Kato S, Yamagishi S, Inagaki Y, Ueda S, Arima N, Okawa T, Kojiro M, Nagata K. Advanced glycation end-products attenuate human mesenchymal stem cells and prevent cognate differentiation into adipose tissue, cartilage, and bone. *J Bone Miner Res* 2005;**20**: 1647–58
33. Babich H, Borenfreund E. Cytotoxicity of T-2 toxin and its metabolites determined with the neutral red-cell viability assay. *Appl Environ Microbiol* 1991;**57**:2101–3
34. Horn P, Bork S, Diehlmann A, Walenda T, Eckstein V, Ho AD, Wagner W. Isolation of human mesenchymal stromal cells is more efficient by red blood cell lysis. *Cytotherapy* 2008;**10**:676–85
35. Anderson ME. Determination of glutathione and glutathione disulfide in biological samples. *Meth Enzymol* 1985;**113**:548–55
36. Kolf CM, Cho E, Tuan RS. Mesenchymal stromal cells—biology of adult mesenchymal stem cells: regulation of niche, self-renewal and differentiation. *Arthritis Res Ther* 2007;**9**:204
37. Liron T, Raphael B, Hiram-Bab S, Bab IA, Gabet Y. Bone loss in C57BL/6J-OlaHsd mice, a substrain of C57BL/6J carrying mutated alpha-synuclein and multimerin-1 genes. *J Cell Physiol* 2018;**233**: 371–7
38. Savion N, Dahamshi S, Morein M, Kotev-Emeth S. S-allylmercapto-N-acetylcysteine attenuates the oxidation-induced lens opacification and retinal pigment epithelial cell death in vitro. *Antioxidants* 2019;**8**:25
39. Weinberg E, Maymon T, Weinreb M. AGEs induce caspase-mediated apoptosis of rat BMSCs via TNF alpha production and oxidative stress. *J Mol Endocrinol* 2014;**52**:67–76
40. Khatri R, Krishnan S, Roy S, Chattopadhyay S, Kumar V, Mukhopadhyay A. Reactive oxygen species limit the ability of bone marrow stromal cells to support hematopoietic reconstitution in aging mice. *Stem Cells Dev* 2016;**25**:948–58
41. Glatt V, Canalis E, Stadmeier L, Bouxsein ML. Age-related changes in trabecular architecture differ in female and male C57BL/6J mice. *J Bone Miner Res* 2007;**22**:1197–207
42. Hung J, Al-Nakkash L, Broderick TL, Castro M, Plochocki JH. Leptin-deficient mice have altered three-dimensional growth plate histomorphometry. *Diabetol Metab Syndr* 2019;**11**:8
43. Ealey KN, Fonseca D, Archer MC, Ward WE. Bone abnormalities in adolescent leptin-deficient mice. *Regul Peptides* 2006;**136**:9–13
44. Williams GA, Callon KE, Watson M, Costa JL, Ding Y, Dickinson M, Wang Y, Naot D, Reid IR, Cornish J. Skeletal phenotype of the leptin receptor-deficient db/db mouse. *J Bone Miner Res* 2011;**26**:1698–709
45. Hamrick MW, Pennington C, Newton D, Xie D, Isaacs C. Leptin deficiency produces contrasting phenotypes in bones of the limb and spine. *Bone* 2004;**34**:376–83
46. Bacevic M, Brkovic B, Albert A, Rompen E, Radermecker RP, Lambert F. Does oxidative stress play a role in altered characteristics of diabetic bone? A systematic review. *Calcif Tissue Int* 2017;**101**:553–63
47. Weinberg E, Maymon T, Moses O, Weinreb M. Streptozotocin-induced diabetes in rats diminishes the size of the osteoprogenitor pool in bone marrow. *Diabetes Res Clin Pract* 2014;**103**:35–41
48. Xia WF, Jung JU, Shun C, Xiong S, Xiong L, Shi XM, Mei L, Xiong WC. Swedish mutant APP suppresses osteoblast differentiation and causes osteoporotic deficit, which are ameliorated by N-acetyl-L-cysteine. *J Bone Miner Res* 2013;**28**:2122–35
49. Hamada Y, Fujii H, Kitazawa R, Yodoi J, Kitazawa S, Fukagawa M. Thioredoxin-1 overexpression in transgenic mice attenuates streptozotocin-induced diabetic osteopenia: a novel role of oxidative stress and therapeutic implications. *Bone* 2009;**44**:936–41
50. Welch AA, Hardcastle AC. The effects of flavonoids on bone. *Curr Osteoporos Rep* 2014;**12**:205–10

(Received February 13, 2022, Accepted March 31, 2022)